

Ultrashort pulse fiber delivery with optimized dispersion control by reflection gratings at 800 nm

Meri Kalashyan,^{1,2} Claire Lefort,² Lluís Martínez-León,³ Tigran Mansuryan,² Levon Mouradian,¹ and Frederic Louradour,^{2,*}

¹ Ultrafast Optics Laboratory, Faculty of Physics, Yerevan State University
1, Alex Manoogian Street, Yerevan 0025, Armenia

² XLIM, Université de Limoges, Centre National de la Recherche Scientifique, UMR 7252,
123 Avenue Albert Thomas, 87060 Limoges cedex, France

³ GROC-UJI, INIT, Universitat Jaume I, Castelló, Spain

*louradour@xlim.fr

Abstract: We experimentally demonstrate a compact and efficient arrangement for fiber delivery of sub-30 fs energetic light pulses at 800 nm. Pulses coming from a broadband Ti:Sapphire oscillator are negatively pre-chirped by a grism-pair stretcher that allows for the control of second and third orders of dispersion. At the direct exit of a 2.7-m long large mode area (LMA) photonic crystal fiber 1-nJ pulses are temporally compressed to 29 fs producing close to 30 kW of peak power. The tunability of the device is studied. Comparison between LMA fibers and standard SMF fibers is also discussed.

©2012 Optical Society of America

OCIS codes: (320.7140) Ultrafast processes in fibers; (230.2035) Dispersion compensation devices; (320.5520) Pulse compression; (260.2030) Dispersion; (140.7090) Ultrafast lasers; (320.7160) Ultrafast technology.

References and links

1. S. A. Crooker, "Fiber-coupled antennas for ultrafast coherent terahertz spectroscopy in low temperatures and high magnetic fields," *Rev. Sci. Instrum.* **73**(9), 3258–3264 (2002).
2. A. T. Yeh, H. Gibbs, J.-J. Hu, and A. M. Larson, "Advances in nonlinear optical microscopy for visualizing dynamic tissue properties in culture," *Tissue Eng. Part B Rev.* **14**(1), 119–131 (2008).
3. Y. Zhao, H. Nakamura, and R. J. Gordon, "Development of a versatile two-photon endoscope for biological imaging," *Biomed. Opt. Express* **1**(4), 1159–1172 (2010).
4. S. J. Im, A. Husakou, and J. Herrmann, "Soliton delivery of few-cycle optical gigawatt pulses in Kagome-lattice hollow-core photonic crystal fibers," *Phys. Rev. A* **82**(2), 025801 (2010).
5. T. Le, J. Bethge, J. Skibina, and G. Steinmeyer, "Hollow fiber for flexible sub-20-fs pulse delivery," *Opt. Lett.* **36**(4), 442–444 (2011).
6. J. S. Skibina, R. Iliew, J. Bethge, M. Bock, D. Fischer, V. I. Beloglasov, R. Wedell, and G. Steinmeyer, "A chirped photonic-crystal fibre," *Nat. Photonics* **2**(11), 679–683 (2008).
7. J. Bethge, G. Steinmeyer, S. Burger, F. Lederer, and R. Iliew, "Guiding properties of chirped photonic crystal fibers," *J. Lightwave Technol.* **27**(11), 1698–1706 (2009).
8. T. Le, G. Tempea, Z. Cheng, M. Hofer, and A. Stingl, "Routes to fiber delivery of ultra-short laser pulses in the 25 fs regime," *Opt. Express* **17**(3), 1240–1247 (2009).
9. P. Tournais, "New diffraction grating pair with very linear dispersion for laser pulse compression," *Electron. Lett.* **29**(16), 1414–1415 (1993).
10. E. A. Gibson, D. M. Gaudiosi, H. C. Kapteyn, R. Jimenez, S. Kane, R. Huff, C. Durfee, and J. Squier, "Efficient reflection gratings for pulse compression and dispersion compensation of femtosecond pulses," *Opt. Lett.* **31**(22), 3363–3365 (2006).
11. T. H. Dou, R. Tautz, X. Gu, G. Marcus, T. Feurer, F. Krausz, and L. Veisz, "Dispersion control with reflection gratings of an ultra-broadband spectrum approaching a full octave," *Opt. Express* **18**(26), 27900–27909 (2010).
12. A. Buettner, U. Buenting, D. Wandt, J. Neumann, and D. Kracht, "Ultrafast double-slab regenerative amplifier with combined gain spectra and intracavity dispersion compensation," *Opt. Express* **18**(21), 21973–21980 (2010).
13. V. Chauhan, P. Bownan, J. Cohen, and R. Trebino, "Single-diffraction-grating and grism pulse compressors," *J. Opt. Soc. Am. B* **27**(4), 619–624 (2010).
14. C. Lefort, T. Mansuryan, F. Louradour, and A. Barthelemy, "Pulse compression and fiber delivery of 45 fs Fourier transform limited pulses at 830 nm," *Opt. Lett.* **36**(2), 292–294 (2011).

15. G. P. Agrawal, *Nonlinear Fiber Optics*, (Academic Press, 2001).
16. M. Moenster, G. Steinmeyer, R. Iliew, F. Lederer, and K. Petermann, "Analytical relation between effective mode field area and waveguide dispersion in microstructure fibers," *Opt. Lett.* **31**(22), 3249–3251 (2006).
17. N. K. T. Photonics, "LMA fiber dispersion overview," http://www.nktpotonics.com/files/files/LMA_fiber_dispersion_overview.pdf
18. C. C. Chang, H. P. Sardesai, and A. M. Weiner, "Dispersion-free fiber transmission for femtosecond pulses by use of a dispersion-compensating fiber and a programmable pulse shaper," *Opt. Lett.* **23**(4), 283–285 (1998).
19. M. Tsang, D. Psaltis, and F. G. Omenetto, "Reverse propagation of femtosecond pulses in optical fibers," *Opt. Lett.* **28**(20), 1873–1875 (2003).
20. S. H. Lee, A. L. Cavalieri, D. M. Fritz, M. Myaing, and D. A. Reis, "Adaptive dispersion compensation for remote fiber delivery of near-infrared femtosecond pulses," *Opt. Lett.* **29**(22), 2602–2604 (2004).
21. Z. Jiang, S. D. Yang, D. E. Leaird, and A. M. Weiner, "Fully dispersion-compensated ~500 fs pulse transmission over 50 km single-mode fiber," *Opt. Lett.* **30**(12), 1449–1451 (2005).
22. N. L. Markaryan, L. K. Muradyan, and T. A. Papazyan, "Spectral compression of ultrashort laser pulses," *Sov. J. Quantum Electron.* **21**(7), 783–785 (1991).
23. L. Kh. Muradyan, N. L. Markaryan, T. A. Papazyan, and A. A. Ohanyan, "Self-action of chirped pulses: spectral compression," *Conf. on Lasers and Electro-Optics US.*, Tech. Dig. CTUH32, 120–121 (1990).
24. M. Oberthaler and R. A. Höpfel, "Spectral narrowing of ultrashort laser pulses by self-phase modulation in optical fibers," *Appl. Phys. Lett.* **63**(8), 1017–1019 (1993).
25. M. Lelek, F. Louradour, A. Barthelemy, and C. Froehly, "Time resolved spectral interferometry for single shot femtosecond characterization," *Opt. Commun.* **261**(1), 124–129 (2006).
26. S. Akturk, M. Kimmel, P. O'Shea, and R. Trebino, "Measuring spatial chirp in ultrashort pulses using single-shot frequency-resolved optical gating," *Opt. Express* **11**(1), 68–78 (2003).
27. D. G. Ouzounov, K. D. Moll, M. A. Foster, W. R. Zipfel, W. W. Webb, and A. L. Gaeta, "Delivery of nanojoule femtosecond pulses through large-core microstructured fibers," *Opt. Lett.* **27**(17), 1513–1515 (2002).
28. S. Ramachandran, J. W. Nicholson, S. Ghalmi, M. F. Yan, P. Wisk, E. Monberg, and F. V. Dimarcello, "Robust, single-moded, broadband transmission and pulse compression in a record A_{eff} (2100 μm^2) higher-order-mode fiber," *ECOC Conf.* **6**, 37–38 (2005).

1. Introduction

Femtosecond optical pulses are now involved in a wide range of applications in science and technology such as, for example, terahertz generation [1] or multiphoton microscopy [2,3]. Frequently it is desirable to deliver those pulses with a flexible optical fiber without losing their basic specificities, i.e. shortness and intensity. However, because of their large bandwidth and high peak power, femtosecond pulses are not easy to deliver with an optical waveguide. They suffer from temporal and spectral broadenings because of respectively group-velocity dispersion and nonlinear self-phase modulation. This is particularly true operating near 800 nm carrier wavelength where normal dispersion is large. Several types of innovative optical fibers were proposed with the aim of reducing the waveguide dispersion or reducing its nonlinearity or more interestingly both of them. An attractive recently published solution relies on a Kagome lattice argon filled hollow-core photonic crystal fiber [4]. Such fiber has a very weak nonlinearity and it has been predicted that its dispersion could be cancelled over a wide bandwidth controlling the pressure of the gas introduced in it. However, the experimental demonstration of this concept is still missing. Up to now the shortest pulse ever delivered by an optical fiber in the 800 nm range has been achieved using an air filled hollow-core fiber with a cladding made of a chirped photonic crystal [5]. This kind of innovative air-silica microstructured fiber has a much larger bandwidth than those of previously experimentally validated hollow-core fibers [6,7]. Its very low and flat dispersion allowed for the delivery of sub-20 fs pulses. However chirped photonic crystal fibers have high guiding losses (> 5 dB/m) so that the previously published result involving this concept provides only 0.13-nJ and 6.5-kW pulses at the output of a relatively short fiber (i.e. 80 cm).

Most applications of femtosecond fiber delivery, such as multi-photon endomicroscopy or fibered femtosecond terahertz generation, require more powerful excitations and longer fibers. T. Le and associates from Femtolasers Produktions GmbH have demonstrated [8] that it was possible to efficiently deliver 800-nm 1.1-nJ 26.5 fs pulses through a 1.6-m long flexible waveguide working with large mode area (LMA) solid-core microstructured fiber. This kind of commercial fiber has a very low attenuation (i.e. < 0.01 dB/m @ 800 nm under

20-cm-bending radius) in addition of being endlessly single mode over a broad bandwidth. It has a small nonlinearity because of a large core. However its dispersion is high so that the key issue relies in this case on fiber dispersion pre-compensation. Dispersion compensation can be achieved by means of an anomalous stretching device located before the fiber compressor. For wide-bandwidth pulses cancellation of only second order dispersion (SOD) is not sufficient; one has to make efforts to compensate also for third order dispersion (TOD). For this reason T. Le worked with a specific SOD and TOD compensation system made of a combination of an expanded two prism-pair or two grating-pair stretcher in combination with two pairs of custom-made TOD optimized chirped mirrors. Authors reported that this scheme was sensitive to chirped mirrors manufacturing tolerances. Additionally this rather complex arrangement was not tunable which is rather detrimental for applications in biophotonics for example. That is why a simpler and cheaper solution for optimized and flexible dispersion compensation is still desirable.

For this purpose we have focused our interest to a solution associating a compact stretcher made of two gratings with a LMA fiber compressor. A grism-pair stretcher is composed of two identical gratings each of them being the assembly of a diffraction grating in close contact with a prism [9]. A grism-based stretcher has a negative SOD and its TOD can be set negative too providing suitable conditions for LMA fiber dispersion cancellation at 800 nm. Inside a grism-pair stretcher there exist enough geometrical freedom degrees to adjust the SOD and TOD continuously and simultaneously at desired values. Conventional prism or grating stretchers do not allow for such optimized dispersion control. It has been demonstrated that grism-pair stretcher is a compact and simple solution for accurate dispersion control. The use of a grism-pair was first proposed for dispersion control by P. Tournois [9] to give high negative SOD with zero TOD. Later, E. A. Gibson and associates [10] showed that a grism-pair can simultaneously compensate for both second and third dispersion orders of material at 800 nm with high throughput working with reflective gratings near Littrow configuration. More recently it has been successfully involved in several ultra-broadband amplified systems [11,12]. Compensation for 10 m of optical fiber at 800 nm has been reported using a compact single-grism compressor [13]. Our group has also recently reported preliminary results about the use of a grism line for fiber delivery and pulse compression [14]. Here we will show that with a grism-pair stretcher it is possible producing 1-nJ pulses with duration well below 30 fs at the direct exit of a 2.7 meter long LMA fiber.

2. Basic features and numerical modelling

Propagation of a femtosecond light pulse inside an optical fiber at 800 nm is mainly governed by chromatic dispersion. In case of nanojoule-pulse Kerr type nonlinearity can also play an important role. The relative impact of those two physical phenomena can be evaluated looking at their respective characteristic lengths. The characteristic length that is associated to

dispersion is $L_D = \frac{\Delta t_0^2}{4 \log 2 \beta_2}$, where Δt_0 is the pulse full width at half maximum in intensity

(FWHM) duration and β_2 the fiber SOD parameter [15]. The dispersion of a LMA fiber is very close to the one of pure fused silica that composes the core with a weak contribution to dispersion coming from the waveguide [16]. At 800 nm β_2 of fused silica amounts to $\approx +35000$ fs²/m so that for a 25-fs pulse L_D is ≈ 6 mm. The nonlinear length is defined as

$L_{NL} = \left[(\omega / c) n_2 \frac{P_{peak}}{A_{eff}} \right]^{-1}$, where $n_2 \approx 3 \cdot 10^{-20}$ m²/W is the nonlinear coefficient and P_{peak} is

the peak power of the pulse and A_{eff} the mode field effective area [15]. For a 1-nJ and 25-fs pulse, propagating in a LMA fiber having a 16- μ m-mode field diameter corresponding to 200- μ m²-mode effective area, the nonlinear length is ≈ 23 mm at 800 nm, meaning that $L_D < L_{NL}$. As a consequence nonlinearity is strongly mitigated by dispersion that becomes the more

important issue that has to be addressed first. As will be discussed later nonlinearity induces some amount of spectral compression but its contribution can be considered as a secondary effect. As a consequence, the performances of the device are mainly related to the accuracy of the balance between the stretcher and the fiber compressor dispersions.

To help to design the stretcher, we have first performed numerical modeling of the [stretcher-compressor] system. Our grism-stretcher is made of an anti-symmetrically positioned reflecting grism-pair (see Fig. 1). Its dispersion has been evaluated as a function of wavelength from group delay geometrical calculation [9]. The following characteristics were used as calculation inputs: (i) for the optical components, grating groove period d , prism apex angle α , prism glass refractive index Sellmeier law $n(\lambda)$; (ii) for the geometrical adjustment freedom degrees (see Fig. 1), incidence angle θ upon the stretcher, distance $L_{\text{prism}} = OT_2$ between the two prisms, distance $L_{\text{tip}} = OT_1$ between the two tips of the two prisms. $L_{\text{in}} = T_1C_1$ is another input parameter; however it can be demonstrated that, at fixed L_{tip} , the value of L_{in} has no impact upon stretcher dispersion.

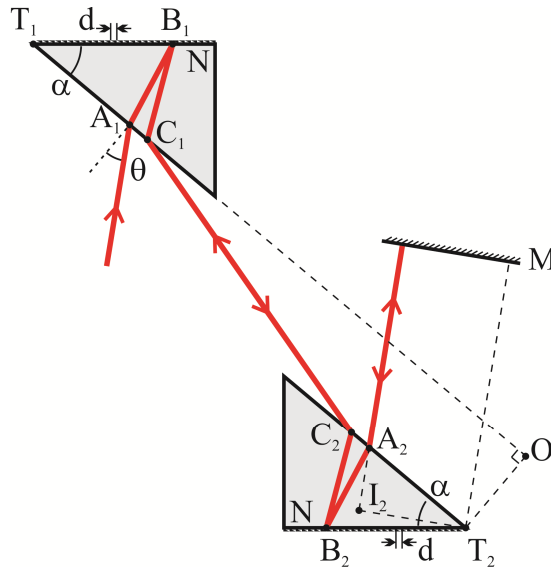


Fig. 1. Monochromatic optical path inside the grism-stretcher. M denotes a retro-reflecting plane mirror. N is the group index of the prism glass, α the prism apex and d the grating groove period and θ the incidence angle. $L_{\text{prism}} = OT_2$ and $L_{\text{tip}} = OT_1$.

The group delay t_g of the stretcher is calculated by adding up the path lengths of an individual frequency component:

$$t_g = \frac{2}{c} [N(A_1B_1 + B_1C_1) + C_1C_2 + N(C_2B_2 + B_2A_2) - A_2I_2]. \quad (1)$$

N is the group index of the prism glass while c denotes the light velocity in vacuum. Path lengths were calculated through conventional laws of optics and geometry. Group delay calculation is an original alternative to spectral phase calculation [11]. Our approach brings equivalent results with the advantage of being more direct.

The dispersive properties of the LMA fiber that plays the role of the compressor were assumed to be the one of pure fused silica (i.e. $\beta_2 = +345.6 \text{ fs}^2/\text{cm}$, $\beta_3 = +282.2 \text{ fs}^3/\text{cm}$ and $\beta_4 = -134.3 \text{ fs}^4/\text{cm} @ 820 \text{ nm}$). The data provided by the manufacturer of the LMA fiber [17] that was used during our experiments confirmed that this assumption is safe. Input temporal and spectral intensity shapes were described with Gaussian functions while durations and bandwidths were measured at half maximum in intensity. Spectral filtering that could result from diffraction grating spectral transmission variation has not been included in the model.

The adjustment of the stretcher begins with the search for the incidence angle θ onto it that provides the suitable ratios $r_{32} = \text{TOD/SOD}$. θ controls $r_{32}^{\text{stretcher}}$ while this ratio is slowly dependent on the distance L_{prism} between the two gratings. In our experiment we worked with gratings made of 600-grooves/mm-gratings and 40°-BK7-prisms. This choice provides the desired r_{32} parameter (i.e. $r_{32}^{\text{stretcher}} = r_{32}^{\text{fused silica}} = +0.817 \text{ fs @ } 820 \text{ nm}$) at $\theta = 38.884^\circ$. In this position the incidence onto the diffraction grating inside the two gratings is equal to 15° . The blaze angle of the grating that has been used during our experiments was 13.9° and the angular deviation induced by the grating is small ($\Delta\theta = \theta_4 - \theta_3 = 12^\circ @ 820 \text{ nm}$) conditions which ensure that the energetic efficiency of the stretcher is high ($>30\%$ across the entire bandwidth).

Now, at fixed θ , SOD and TOD of the stretcher increase approximately linearly with distance L_{prism} between the two gratings so that the desired SOD and TOD can be reached simultaneously adjusting L_{prism} . During our experiments we worked with a 2.7-meter-long LMA fiber having $\varphi_2^{\text{fiber}} = +9.332e+4 \text{ fs}^2$, $\varphi_3^{\text{fiber}} = +7.627e+4 \text{ fs}^3 @ 820 \text{ nm}$. The fiber SOD and TOD cancellations are performed simultaneously at $\theta = 39.884^\circ$ with $L_{\text{prism}} = 14.404 \text{ mm}$ and $L_{\text{tip}} = 59 \text{ mm}$. In this position the [stretcher-compressor] is limited by uncompensated higher orders of dispersion. Calculations revealed that fourth order of dispersion (FOD) was the limiting factor with a negligible impact coming from the fifth and higher orders. Stretcher and fiber FODs amounted respectively to $\varphi_4^{\text{stretcher}} = -4.42e+5 \text{ fs}^4$ and $\varphi_4^{\text{fiber}} = -3.64e+4 \text{ fs}^4 @ 820 \text{ nm}$. The two contributions have the same sign meaning that they cannot compensate for each other and the net FOD is largely dominated by the stretcher contribution. When applied to a signal with 50-nm-bandwidth it results in a pulse with duration equal to 40 fs (see Fig. 2(a)) which is twice the Fourier limit (i.e. 19.4 fs for a Gaussian shape pulse having a 50-nm-bandwidth). Changing for a grating with a different groove density and/or for a prism with a different apex and/or material could represent solutions for smaller FOD while preserving SOD and TOD cancellations. However our calculations showed that those alternative choices could result in large deviations from the Littrow configuration inside the gratings and as a consequence to deleterious reduction of the stretcher throughput. The above mentioned parameter set involving readily available commercial components (see next section) represents a good trade-off between optimized dispersion compensation with moderate FOD and high throughput.

Else, exact cancellation of the net SOD is not optimum in term of compressed pulse duration. Indeed it is advantageous to work with some amount of positive net SOD (i.e. $+620 \text{ fs}^2$ in the particular conditions that were described above) that is able to partially mitigate the negative net FOD coming namely from the grism-stretcher. Calculations confirm that a significantly shorter and brighter pulse can be obtained for different adjustments of the stretcher. The minimal duration is obtained with $\theta = 38.925^\circ$ and $L_{\text{prism}} = 14.385 \text{ mm}$. It amounted to 26.6 fs (FWHM) (see Fig. 2(c)) which corresponds to 1.4 times the Fourier limit while the peak power exceeds 30 kW for a 1-nJ pulse which corresponds to 62% of the peak power of the Fourier transformed pulse having identical bandwidth and energy. In case of exact cancellation of net SOD, a 1-nJ pulse having the same bandwidth has a peak power amounting to only 19 kW.

In the same conditions (i.e. with the same fiber, the same bandwidth, the same pulse energy), working with a grating-pair stretcher would relate to a delivered pulse with a much larger duration (i.e. 3 times larger for 600 grooves/mm gratings separated by 12.5 cm).

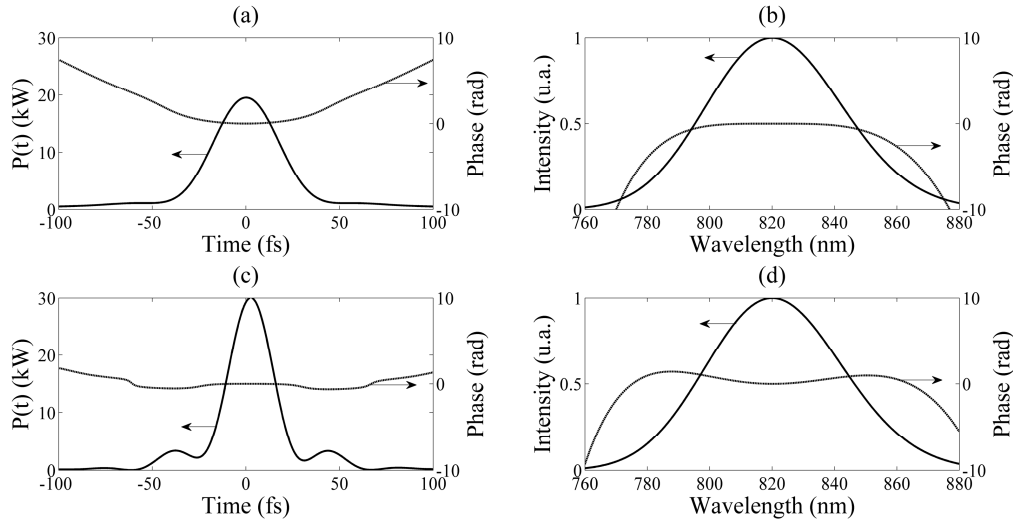


Fig. 2. Calculated pulses and spectra at the direct output of 2.7-m long LMA fiber for two different adjustments of the grism-based stretcher at fixed $L_{\text{tip}} = 59$ mm. (a) and (b): $\theta = 39.884^\circ$ and $L_{\text{prism}} = 14.404$ mm; the stretcher perfectly compensates for both SOD and TOD of the fiber while a net uncompensated FOD (i.e. $-4.79e + 5 \text{ fs}^4$) can be seen on (b); the compressed pulse duration is equal to 40 fs (FWHM) with a peak power amounting to 19 kW for a 1-nJ pulse - (c) and (d): $\theta = 38.925^\circ$ and $L_{\text{prism}} = 14.385$ mm; now the stretcher is adjusted so that TOD is compensated and that net SOD and net FOD partially compensate for each other; spectral phase variation amplitude across the spectrum is somewhat smaller, as a consequence the pulse duration is smaller (i.e. 26.6 fs) and the peak power is higher (i.e. more than 30 kW for a 1-nJ pulse).

Because of very high uncompensated TOD, numerous secondary pulses would appear in the trailing edge of the compressed pulse. The peak power and the ability of producing at the fiber exit a second order nonlinear signal, such as two-photon fluorescence, would be respectively 6 and 9 times smaller. Working with a prism-pair stretcher would result in very similar performances in comparison with gratings, except for the secondary pulses that would appear now in the leading edge, but with the additional drawback of requiring a very large distance between the two components (i.e. more than 2 meters between two SF11 prisms inside a 4-pass-stretcher).

Our device gives also very interesting results with long fibers [18–21]. For example we have performed simulations increasing the fiber length to 10 meters (i.e. 3.7 times the previous one), all other characteristics being unchanged. With this long fiber SOD and TOD exact cancellations were obtained for the following parameters: $L_{\text{prism}} = 61.21$ mm, $\theta = 39.48^\circ$ and $L_{\text{tip}} = 150$ mm. In this situation the stretcher FOD increased by a factor 3.2 (i.e. $\varphi_4^{\text{stretcher}} = -1.4e + 6 \text{ fs}^4$) with respect to the case of a 2.7-meter-long fiber what resulted in a longer compressed pulse. However the delivered pulse is still very short. Its duration amounted to 57 fs (FWHM) which is only 1.4 times longer than the one for the 2.7-meter-long fiber and the pulse shape was unchanged. As previously, the shortest pulse has been performed when SOD partially mitigated FOD. It was obtained when $L_{\text{prism}} = 61.15$ mm and $\theta = 39.50^\circ$ and the shortest duration amounted to 34 fs (FWHM) at the end of the 10-meter-long LMA fiber.

Now it is important to check that the performances of our [stretcher-compressor] device are preserved at high power when nonlinear effects happen in the last few centimeters of the fiber compressor. For this purpose the nonlinear pulse propagation inside the dispersive LMA fiber has been modeled using the split-step method proposed by G.P. Agrawal [15]. Our model accounts for dispersion at all orders coming from the grism-based stretcher and from

the fiber, for Kerr self-phase modulation, self-steepening and Raman scattering coming from fused silica third order optical nonlinearity inside the fiber core. At the largest energy level that has been achieved experimentally (i.e. 1 nJ at the fiber exit), the calculated total nonlinear phase-shift amounted to $\approx\pi/2$ radians meaning that nonlinear effects do have some impact. At this power level we have observed numerically and experimentally a noticeable spectral compression at the fiber exit amounting to 18% of the initial spectral width. However the compressed pulse duration does not increase proportionally as it would be the case for a Fourier limited compressed pulse. For a 1-nJ-pulse exiting the LMA fiber, the final duration increases to only 27.4 fs corresponding to a 3%-increase with respect to the linear regime. In presence of nonlinearity the calculated peak power amounted to 26 kW. This can be understood as follows; because it acts upon negatively chirped pulse, nonlinearity removes frequencies in the spectrum wings resulting in spectral compression [22–24] instead of more common spectral broadening when acting upon unchirped pulse. Those lateral spectral components are more affected by FOD. That is why, by removing the spectral components that are affected the most by FOD, nonlinearity somehow tends to reduce the negative impact of FOD. Simulations reveal that self-steepening has a negligible impact while Raman scattering induces slight spectral modulations in the summit of the spectrum without modifying the pulse shape in a noticeable manner. As a conclusion we can confirm that the system is weakly influenced by nonlinearity of a LMA fiber. The scalability of the device to higher energy levels and the use of more nonlinear fibers with smaller core such as standard SMF will be discussed below.

3. Stretcher-compressor implementation

We started from a commercial femtosecond Ti: Al₂O₃ broadband oscillator (MICRA-5 from COHERENT, Inc.) having the following parameters of radiation: adjustable spectral bandwidth from 20 nm to 110 nm; 80 MHz for the repetition rate; 400 mW average power; 805 nm central wavelength in case of 110-nm-bandwidth; central wavelength tunable in the range of 750-850 nm @ 20-nm-bandwidth; rectilinear polarization within the setup plane. At the direct output of the MICRA oscillator the pulse is not compressed ($\phi_2^{MICRA\ oscillator} \approx +500\text{ fs}^2$, $\phi_3^{MICRA\ oscillator} \approx +400\text{ fs}^3$). However it is rather negligible with the dispersions induced later by the grism-based stretcher and by the fiber. The pulses emitted by this femtosecond source were negatively stretched by our grism-based stretcher that was made of two home-assembled grisms before being launched into the delivery fiber (see Fig. 3). Each grism was composed of a 40° antireflection coated BK7 (ref. H-K9L from Union Optics) prism separated by a 30 μm air gap from a 600 grooves/mm gold coated blazed diffraction grating from Richardson Gratings (ref. 53066BK02-351R).

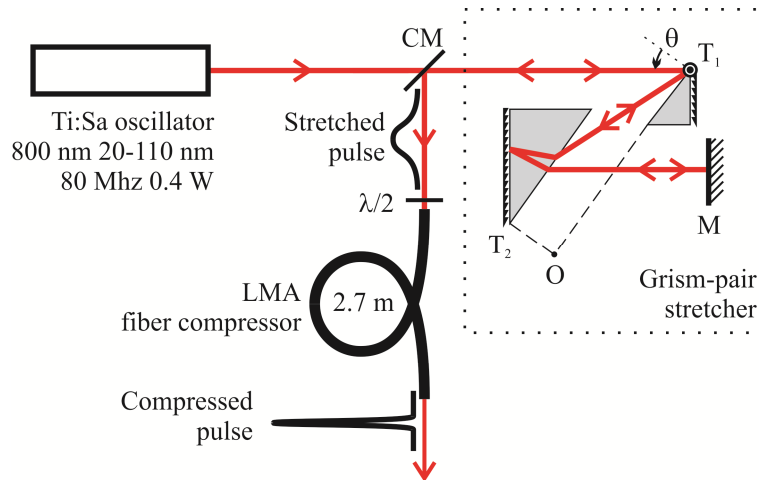


Fig. 3. Experimental setup. The system was composed of three main elements: a Ti:Sa femtosecond oscillator, an anomalous stretcher made of two antiparallel gratings each of them being the assembly of a prism in close contact with a reflective diffraction grating, and a 2.7-meter-long large mode area microstructured (LMA) fiber. The stretcher was adjusted so that the pulse was optimally compressed at the direct exit of the LMA fiber. The main freedom degrees are θ , $L_{\text{Prism}} = OT_2$ and $L_{\text{Tip}} = OT_1$; CM \equiv cut mirror; M \equiv plane retro-reflecting mirror.

The stretcher had a net energetic efficiency amounting to 36% (i.e. 78% for one grism) for an incident rectilinear polarization within the setup plane. The total spatial footprint of the device is equal to 100 cm^2 . Then light was launched into a 2.7 meter long endlessly single-mode LMA fiber from THORLABS, Inc. (ref. LMA-20) that has been cleaved by ourselves. A self-made cleave mostly produces a small angle ($1\text{-}2^\circ$) between the normal of the fiber input face and the incoming beam, which deflects the reflected beam enough to not disturb significantly the oscillator anymore. For this reason there was no isolator within the setup, nevertheless we have never had problem of reinjection in the oscillator. The pure fused silica core of the LMA fiber had a mode field radius equal at $1/e$ to $8.3 \mu\text{m}$ (i.e. an effective mode field area equal to $215 \mu\text{m}^2$) with a low numerical aperture equal to $0.04 @ 780\text{nm}$. An achromatic lens with $f = 15\text{mm}$ for its focal length served to inject light into the fiber with a coupling efficiency amounting to 68% at best. The LMA was not polarization maintaining but it was slightly birefringent. A half-wave plate was located before the fiber in order to excite only one polarization mode. At the exit the polarization was approximately rectilinear. The fiber bending radius was equal to 30 cm so that the fiber transmission was close to 100%. As a result, the energy of the pulse that exited the fiber could reach at best 1 nJ. After the fiber a noncollinear second order autocorrelator with a $10\text{-}\mu\text{m}$ -thin doubling crystal and an interferometric autocorrelator with a two-photon-absorption photodiode were used for temporal characterizations while an optical spectrometer performed simultaneous spectral analysis. Coherent pulse measurements were also performed by using time resolved spectral shearing interferometry through SPIRIT [25] that has been specially adapted to broadband pulses.

4. Experimental results

The best result that we have obtained experimentally is reported in Fig. 4, proving the delivery of pulses having sub-20-fs duration and 1-nJ energy at the direct exit of a 2.7-meter-long LMA fiber.

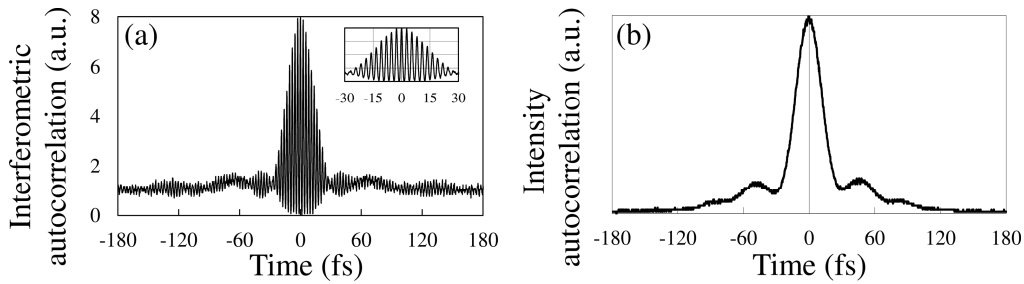


Fig. 4. (a): Interferometric autocorrelation. (b): Intensity autocorrelation indicate very short durations for 1 nJ pulses at the direct exit of a 2.7-meter-long LMA fiber. Both of the two autocorrelations are related to sub-20-fs (FWHM) duration (respectively 17.8 fs and 19.9 fs for secant hyperbolic square and Gaussian shape pulses).

The corresponding output spectrum width was equal to 51 nm. The actual time-bandwidth product amounted to 0.46 assuming Gaussian shape pulse. The Fourier-transform limited pulse having the same spectrum and the same energy (i.e. 1 nJ) would correspond to 48-kW-peak power. We have estimated that the pulse peak power was in the range of 30–40 kW. The previous pulse duration is notably smaller than calculation predictions (see Fig. 2(c)). This could be explained perhaps by the fact that our broadband oscillator (MICRA from COHERENT, Inc.) could deliver highly chirped pulses. There exists a specific laser operation regime during which a large positive FOD imparts the emitted pulse. In this situation the oscillator could contribute to strongly reduce the uncompensated FOD of the whole system.

During more common operation regimes (e.g. just after cleaning and/or readjusting the laser cavity) the oscillator FOD returns to moderate values so that this contribution vanishes. In those more usual and more reproducible cases, we have measured sub-30-fs pulses accordingly to what was predicted by the model (see Fig. 2(c)). The compressed pulse duration was equal to 29 fs (FWHM) what corresponded to 0.65 for the time-bandwidth product.

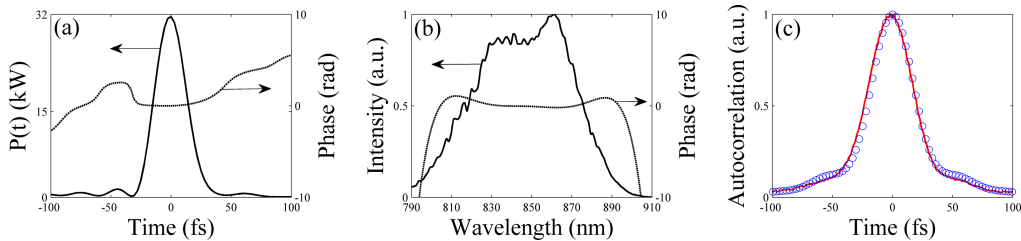


Fig. 5. (a) and (b): Coherent pulse characterization performed through SPIRIT (Spectral Interferometry Resolved In Time) at the exit of a 2.7-meter-long LMA fiber for 1-nJ pulses. Pulse duration amounted to 29 fs (FWHM) with 31.6-kW peak power; (c) red solid line: Autocorrelation measured with a non collinear second order autocorrelator – blue circles: calculated autocorrelation from SPIRIT trace. Those results were obtained without contribution to dispersion coming from the oscillator.

Coherent pulse characterization using SPIRIT apparatus [25] allows us to retrieve the spectral phase shape (Fig. 5(b)) predicted by the numerical model (see Fig. 2(d)). The delivered pulse has a clean shape with 29-fs-duration (FWHM) and more than 30-kW-peak power.

At the direct exit of the laser, the initial spectrum width was 71 nm. After the grism-stretcher it was 62.5 nm. At the LMA fiber exit, in case of low power the bandwidth was equal to 62.5 nm, while in case of high power it was reduced to 51 nm (see Fig. 6) corresponding to 18% spectral compression.

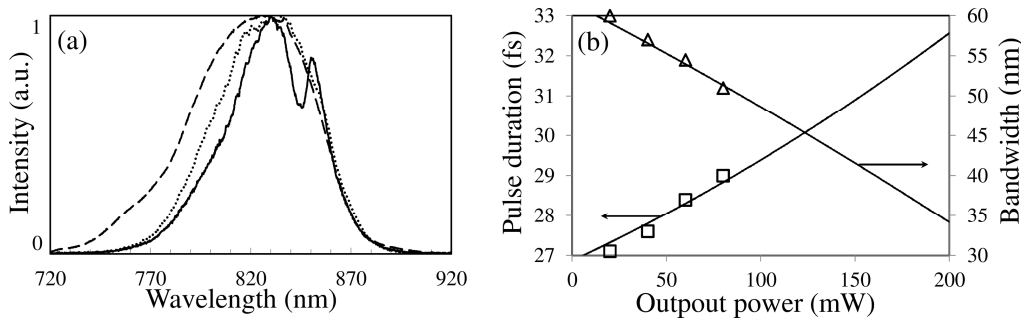


Fig. 6. (a): Spectral densities at the oscillator output (red line), at the grism-stretcher output (green line) and at the LMA-PC fiber output (black line) for 1 nJ pulses. For those three locations the bandwidths were respectively equal to 71 nm, 62.5 nm and 51 nm. Grism-stretcher filtering and spectral compression coming from nonlinear propagation inside the fiber are the reasons for bandwidth variations. (b): Pulse duration and spectral bandwidth at the output of the 2.7-meters-long LMA fiber as a function of output power. Triangle and square represent experimental measurements while solid lines relate to calculations.

The red-shifting filtering effect introduced by the grism-stretcher (see Fig. 6(a)) can be attributed to the grating spectral transmission. At low power, the spectrum exiting the fiber is close to the one at the fiber input. It proves the high spatial quality of the beam exiting the grism-stretcher which is exempt from spatial and angular chirp [26]. In order to study the spectral compression inside the LMA fiber, we have registered bandwidths for different power levels at the exit of the LMA fiber. Spectral compression is clearly seen on Fig. 6(b).

The MICRA oscillator which is bandwidth adjustable offers the opportunity to investigate the influence of the initial spectral bandwidth. Figure 7 reports pulse intensity autocorrelations for different initial spectral bandwidths. For narrow bandwidths, dispersion is easily compensated leading to clean Fourier transform limited compressed pulses. In this case the pulse is long (i.e. 55 fs @ 20-nm-bandwidth). For broad bandwidths, time aberrations coming from uncompensated FOD distort the signal which contains satellite pulses. The shortest autocorrelation duration has been obtained in case of 70 nm spectral bandwidth (see Fig. 7(b)).

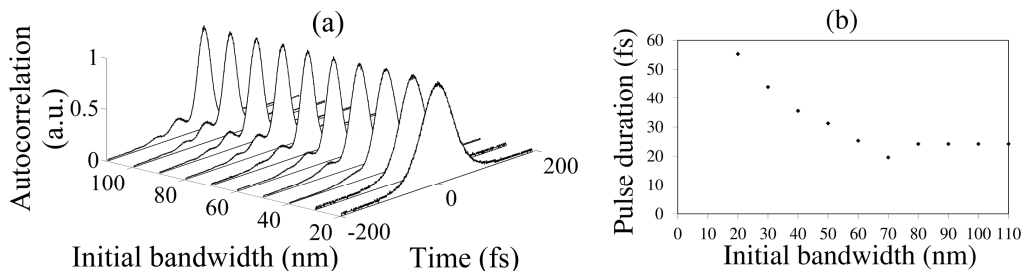


Fig. 7. (a): Intensity autocorrelations at the output of a 2.7 m long LMA fiber for 1 nJ pulses @ 820 nm for different initial bandwidths emitted by the oscillator that fed the device. (b): 70 nm for the initial bandwidth appear to be the optimum in terms of pulse shortness and brightness.

Carrier frequency tuning of our fiber delivery system has also been investigated. This study has been performed working with 20-nm-bandwidth pulses what allowed us to tune the carrier wavelength over 100 nm (see Fig. 8). This wide tunability is an advantageous feature namely towards biomedical applications for which optimization of operating wavelength is an important issue.

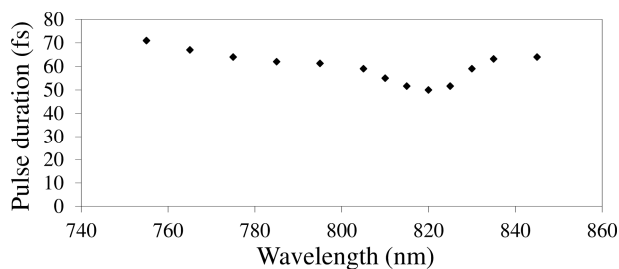


Fig. 8. Output pulse duration as a function of carrier wavelength varying across the full tunability range (i.e. 100 nm) of our MICRA-5 oscillator when adjusted with 20-nm-bandwidth. The tunability of our femtosecond fiber delivery system expands across more than 100-nm-bandwidth from 750 to 850 nm. The optimal carrier wavelength in terms of pulse shortness appeared to be equal to 820 nm.

Despite the advantageous feature of being weakly nonlinear because of their large core, LMA fibers offer poor spatial resolution when used inside an imaging device such as a multiphoton endomicroscope [3]. This is true for air-silica microstructured LMA fibers [27] and also for higher-order-mode LMA fibers [28] that were also successfully involved in powerful femtosecond pulse fiber delivery demonstrations. From the point of view of spatial resolution, standard single mode fibers (SMF) with small fundamental mode size could be preferred. In order to prove that our dispersion compensation scheme also brings benefits with this kind of more nonlinear fibers, we replace the LMA fiber by a standard single mode fiber having 6- μm -mode field diameter corresponding to 28- μm^2 -mode effective area. This type of fiber is approximately 7 times more nonlinear than the LMA-20 that was used during our previous experiments, while its SOD is 1.2 times greater (i.e. $\beta_2 = +392 \text{ fs}^2/\text{cm}$; $\beta_3 = +320 \text{ fs}^3/\text{cm}$ and $\beta_4 \approx -150 \text{ fs}^4/\text{cm}$ @ 820 nm). For a 1-nJ-energy 25-fs-duration pulse propagating in it, the nonlinear length is $L_{\text{NL}} = 6 \text{ mm}$ what leads to $L_{\text{D}} \approx L_{\text{NL}}$ (see section 2.). Dispersion is still mitigating nonlinearity but in a smaller extent than in the case of LMA fiber where $L_{\text{D}} \ll L_{\text{NL}}$. Some nonlinear spectral compression is now predicted at the SM fiber exit. However it is much smaller than in the case of narrowband pulses [27] which relate to $L_{\text{D}} \gg L_{\text{NL}}$. For this reason, we have obtained short compressed pulses at the output of the SM fiber too. By using a 2.7-meters-long standard polarization maintaining single mode fiber (PM-SMF), in case of 820 nm carrier wavelength, for a 60-nm initial bandwidth and 80-mW power injection (i.e. 1-nJ-energy delivered pulse) we have recorded autocorrelation with 39-fs-duration corresponding to Gaussian pulse with 28-fs-duration (see Fig. 9). In this situation spectral compression inside the standard SMF amounted to 36%.

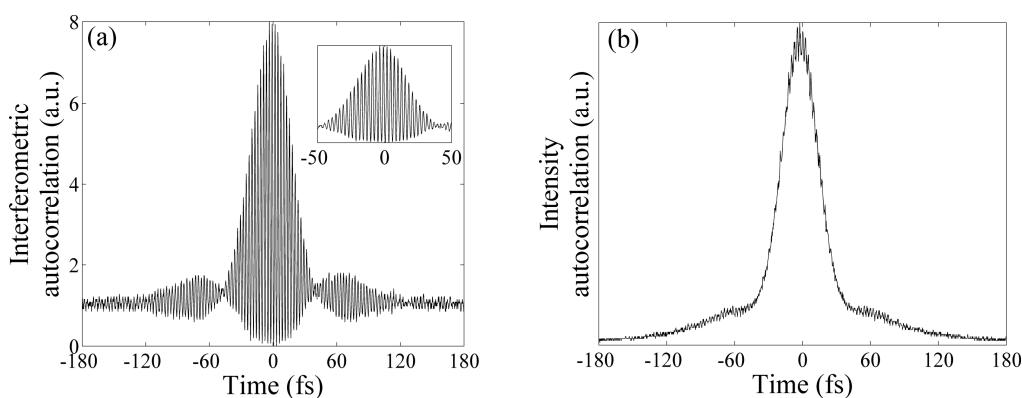


Fig. 9. Pulse delivered at the output of a 2.7-meters-long standard PM-SM fiber. Interferometric (a) and intensity (b) autocorrelations are both related to 28-fs-duration (FWHM) pulse having 1-nJ-energy.

As in case of LMA fiber, the shortest pulse durations were measured during the particular operation regime during which the laser oscillator brought a non-negligible contribution to FOD. Without this favorable circumstance we have obtained 32.5-fs-duration pulses having 1-nJ-energy. Comparison between LMA and PM-SM fibers and scalability to higher power levels are evidenced on Fig. 10. With the standard SMF spectral compression is much stronger (see Fig. 10(b)) and the pulse is longer with a more complex shape (see Fig. 10(c)). However it is worth noticing that even at energy levels as high as 2.5 nJ the pulse duration is still much smaller than 50 fs at the output of the standard SMF.

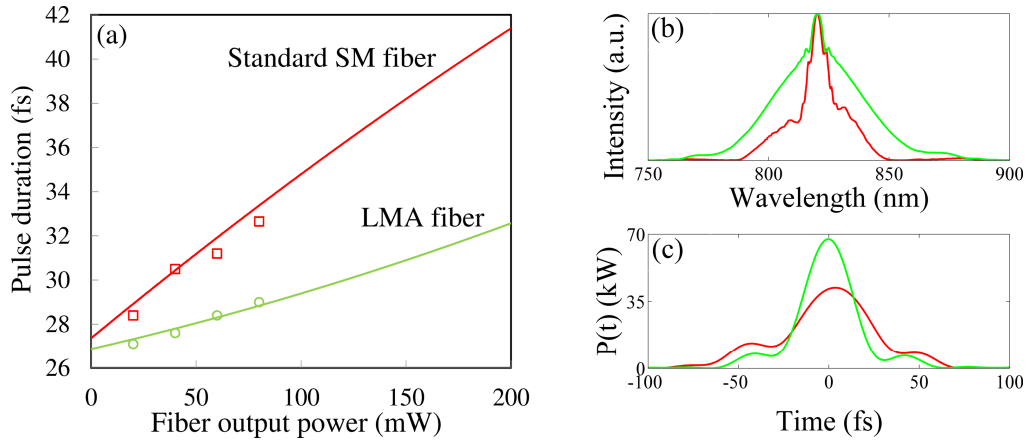


Fig. 10. (a): Measured pulse duration as a function of output average power at the output of a 2.7-meter-long fiber, red squares with a standard PM-SM fiber, green circles with a LMA fiber. Solid lines are corresponding calculations (red line for the standard SMF and green line for the LMA SMF). (b): Calculated spectra at the fiber exit for 200 mW average power @ 80 MHz (i.e. 2.5 nJ). Spectral compression is much stronger in the standard SMF (red line) which has increased nonlinearity. (c): Calculated pulse temporal profiles. LMA SMF (green line) gave a cleaner and brighter pulse.

5. Conclusion

We have numerically and experimentally demonstrated an efficient femtosecond fiber delivery setup with improved fiber dispersion precompensation thanks to a high throughput grism-pair stretcher. Sub-30-fs-duration 1-nJ-energy pulses were compressed at the direct exit of 2.7-meters-long large mode area fiber. The proposed device that involves only readily available commercial components is compact in addition of being wavelength tunable over a 100-nm-bandwidth around 800 nm. Large mode area fibers gave the best performances in terms of pulse shortness and brightness. But surprisingly standard single mode fibers also gave short and powerful pulses despite their increased nonlinearity.

Acknowledgments

We warmly thank M. Pierre Tournois for his fruitful help during grism stretcher modelling. This work is supported by the French “Agence Nationale de la Recherche” (ANR) project Invivo-ONL and by the CNRS-SCS Armenia-France funding.